mated from models (*9*) and measured directly (*10*). These measurements indicate that the altitude region from 25 to 30 km is nearly saturated with a vapor concentration of 10^5 to 10^6 molecules per cubic centimeter. Thus, after a major volcanic eruption, which injects large amounts of sulfurous gases to the 25-km region (as El Chichón apparently did), a high degree of H_2SO_4 supersaturation can evolve in this region. Under such conditions two things, important for particle formation in the stratosphere, can happen. (i) If the supersaturation is high enough (H_2SO_4 concentration exceeds $\sim 10^7$ molecules per cubic centimeter at 25 km), H_2SO_4–H_2O droplets will form homogeneously from the gas phase (*11*), that is, do not require a condensation center. (ii) Accretion of the vapor and the newly formed droplets on existing particles will cause substantial growth of the preexisting distribution of particles.

Creation of new droplets under supersaturated conditions is a very rapid and copious process, resulting in high particle concentrations ($\gtrsim 10^3\ cm^{-3}$) initially. However, since the coagulation rate depends on the square of the concentration, the coagulation of droplets takes place very rapidly. As the size of the coagulating droplets increases, the concentration decreases rapidly and the lifetime increases. Under such conditions the smallest particles are rapidly depleted; this results in a maximum in the particle size distribution. The distribution so formed approximates a log-normal distribution (*12*), as we have observed. Thus our interpretation of the observed bimodal distribution as representing new droplet nucleation on the one hand and growth of the preexisting distribution on the other is consistent with what is known about such stratospheric processes.

The fact that the August and October 1-μm particle concentrations observed over Texas at 25 km were very similar and that the total mass was relatively constant indicates that, although no new particles were being created during this period, particles lost as a result of gravitational settling were replaced through growth of smaller particles. Since particles with $r \lesssim 0.05$ μm had essentially disappeared as a result of coagulation by August, replenishment of the 1-μm droplets probably occurred primarily through molecular accretion on particles in the 0.3-μm mode. With this assumption, one can estimate the H_2SO_4 concentration. For kinetically limited growth in the low-pressure limit, one may obtain the rate of change of the droplet radius by equating the molecular mass flux on a particle's surface with the rate of change of mass of the particle

$$\frac{dr}{dt} = \frac{1}{4} v V n_a$$

where v is the molecular thermal velocity, V is the molecular volume, and n_a is the H_2SO_4 molecular concentration in excess of the saturation concentration. Growth from 0.3 to 1 μm in 100 days (the time required for a 1-μm particle to fall from 25 to 18 km) gives an H_2SO_4 concentration of about 10^7 molecules per cubic centimeter.

The loss rate of vapor to a distribution of particles is given by the molecular flux on a surface multiplied by the total particle surface area

$$\frac{dn_a}{dt} = -\frac{1}{4} v n_a \int_0^\infty 4\pi r^2 n(r) dr$$

Thus the exponential time constant for vapor loss is given by

$$\tau = \left[\pi\, v \int_0^\infty r^2 n(r) dr\right]^{-1}$$

For the size distribution observed in May, τ had a value of only about 5 minutes, whereas in August and October it had lengthened somewhat to 15 to 20 minutes. This result suggests that the vapor would be rapidly used up (would be down by a factor of 100 in 4.6 time constants) by the particles if it were not replenished. Thus the conversion from volcanic sulfurous gas to H_2SO_4 must have taken place continuously.

Measurements at Laramie through December 1982 indicate a continual growth of the total mass in the stratosphere. Thus the normal "decay" of the event, which for past eruptions had an exponential time constant of about 10 months (*3*), had not yet begun. The El Chichón eruption of 1982 is the largest such event, in terms of lasting effects on the stratosphere, since the advent of stratospheric measurements and probably will prove to be the largest in at least the past century.

D. J. Hofmann
J. M. Rosen
Department of Physics and Astronomy, University of Wyoming, Laramie 82071

References and Notes

1. D. J. Hofmann, J. M. Rosen, T. J. Pepin, R. G. Pinnick, *J. Atmos. Sci.* **32**, 1446 (1975); J. M. Rosen and D. J. Hofmann, *J. Appl. Meteorol.* **16**, 56 (1977).
2. D. J. Hofmann and J. M. Rosen, *J. Geophys. Res.* **87**, 11,039 (1982).
3. ———, *ibid.* **82**, 1435 (1977).
4. ———, *Geophys. Res. Lett.* **8**, 1231 (1981).
5. K. Labitzke, B. Naujokat, M. P. McCormick, *ibid.* **10**, 24 (1983).
6. D. J. Hofmann and J. M. Rosen, *J. Atmos. Sci.* **38**, 168 (1981).
7. J. Deluisi, E. Dutton, B. Mendonca, M. King, *Eos* **63**, 897 (abstr.) (1982); K. L. Coulson, T. E. Defoor, J. Deluisi, *ibid.*, p. 897 (abstr.).
8. D. J. Hofmann and J. M. Rosen, *Geophys. Res. Lett.* **10**, 313 (1983).
9. R. P. Turco, O. B. Toon, P. Hamill, R. C. Whitten, *J. Geophys. Res.* **86**, 1113 (1981).
10. A. A. Viggiano and F. Arnold, *Geophys. Res. Lett.* **8**, 583 (1981).
11. G. K. Yue and A. Deepak, *J. Geophys. Res.* **87**, 3128 (1982).
12. G. C. Lindauer and A. W. Castleman, Jr., *Nuc. Sci. Eng.* **43**, 212 (1971).
13. This research was supported by the National Science Foundation, the National Aeronautics and Space Administration, the Office of Naval Research, and the Air Force Geophysics Laboratory.

20 January 1983; revised 25 April 1983

Zonal Winds in the Central Equatorial Pacific and El Niño

Abstract. *Easterly trade winds from near-equatorial islands in the central Pacific weakened before each El Niño between 1950 and 1978, except for the 1963 El Niño. The weakening of the easterlies and their later collapse did not occur uniformly over several months, but rather through a series of strong westerly wind bursts lasting 1 to 3 weeks. The bursts may force equatorial Kelvin waves in the ocean that can both initiate and sustain the sea surface warming characteristics of El Niño events.*

The term El Niño commonly refers to the occurrence of unusually warm surface water near the coast of South America just south of the equator (*1, 2*). As part of the southern oscillation (*2*), El Niño precedes or coincides with anomalous oceanographic (*3*) and meteorological (*2*) conditions throughout the tropical Pacific, and has been related to mid-latitude weather (*4*). The exact sequence of events and the physical mechanisms of their interaction are subjects of increasing research and debate. We examine here some newly acquired time series of wind data from central Pacific islands and relate the zonal wind fluctuations to El Niño events.

Wyrtki (*3*) suggested that El Niño events follow a strengthening and subsequent weakening of the trade winds over the central equatorial Pacific. Theoretically, the effect of these wind changes on the ocean can be quickly propagated eastward by equatorial waves (*5, 6*). The connection between the propagation of these waves and changes in sea surface temperature (SST) is not completely understood, but SST anomalies can be caused by nonlinear advection (by the equatorial waves) of the horizontal gradients of the existing temperature field (7, 8).

The observational connection between precursive wind anomalies and El Niño is ambiguous. The time and space structure of the precursive wind anomaly over the central Pacific is not well established; even the existence of such an anomaly has been questioned (2, 7). Recent analyses of merchant marine weather data suggest precursive zonal wind anomalies that extend over quite different regions west of the date line near the equator (2, 9). But these analyses lump all the El Niño events together, ignoring the variability between events or not distinguishing between the different phases of El Niño events (10). Wyrtki (3) noted that "weaker winds in the central equatorial Pacific occur about simultaneously or slightly after El Niño has commenced." The difficulty of observing the precursive wind anomaly arises from the incompleteness of the data obtained by merchant marine vessels (11). However, Busalacchi and O'Brien (12) had some success in modeling aspects of the El Niño sea level signal in the east with a reduced-gravity numerical model of the equatorial Pacific that utilizes monthly means of the merchant marine wind observations.

Our study, which is based on wind measurements at island stations, tends to support Wyrtki's (3) hypothesis to the extent that the easterly winds near the equator between 170°E and 170°W strengthened and then relaxed before the first positive SST anomalies off Peru for most El Niño events between 1950 and 1978. The island data show, however, that the relaxations did not occur uniformly over several months, but rather tended to begin as a series of closely spaced, energetic, westerly wind bursts of short duration (1 to 3 weeks) (13). Throughout the El Niño years, even during the mature phase when the relaxation of the easterly trades is most extensive (2), we find much of the low-frequency westerly anomaly to be due to frequent westerly wind bursts.

We describe here surface winds measured at two islands of the Gilbert group (Tarawa, 1°21'N and 172°55'E, and Ocean, 0°54'S and 169°32'E) and one of the Phoenix group (Canton, 2°46'S and 171°43'W). Tarawa and Canton are coral atolls with anemometers, and Ocean is a small, nearly circular island (maximum elevation, about 80 m) from which the Beaufort force of the winds was estimated. Tarawa's anemometer was 39 m above sea level (at least 12 m above the tree tops) and Canton's anemometer was 9 to 12 m above sea level (above the sparse vegetation). The stations are on the southwest (Tarawa and Ocean) or northern (Canton) sides of the islands. The climatological wind is predominantly easterly at each island. The stations supplied 3 to 24 observations per day, averaging 6. We believe that these wind observations are as representative of open ocean conditions as is possible for routine weather observations from islands. The similarity of their power spectra and low-pass-filtered winds support this belief (11).

The low-pass-filtered (14) zonal wind anomalies from Ocean, Tarawa, and Canton are plotted in Fig. 1. The visually striking westerly (positive) anomalies are associated with El Niño events. Following Quinn *et al.* (15), we classify the 1950–1978 El Niño events as strong (1957 to 1958, 1972 to 1973), moderate (1953, 1965 to 1966, 1976 to 1977), weak (1951 and 1969), and very weak (1963 and 1975). In addition, there is evidence (16, 17) that 1979 to 1980 should be considered a weak El Niño period. (Hereafter, multiyear events will be referred to by the first year only.) The definitions above have identified almost all the years with low-frequency westerly anomalies in Fig. 1 as El Niño years. However, the strength of the wind anomaly does not always correspond to the strength of El Niño.

The dates of the first occurrence of warm SST anomalies at the coast of South America for each El Niño except that of 1979 are indicated in Fig. 1 (3, 18–20). The low-frequency easterly winds relax by 1.5 to 4.0 m sec^{-1} (and westerly anomalies occur) at one or more of the three stations 1 to 4 months before the first SST maximum for each El Niño except that of 1963. The precursive zonal wind changes at Canton appear to be weaker than in the Gilbert Islands for two (1953 and 1965) of the El Niño events in 1950 to 1967, and stronger for two others (1951 and 1957). There is a suggestion of westward propagation of the precursive wind anomaly for the 1957 El Niño (Canton to Tarawa to Ocean) and eastward propagation for the 1965 El Niño. The 1- to 4-month lag of the SST anomalies is consistent with Kelvin wave propagation (first or second baroclinic mode) of the wind signal from the Gilbert Islands to South America (21). Luther and Harrison (11) suggested that the 1963 El Niño was initiated by (observed) meridional wind anomalies in the

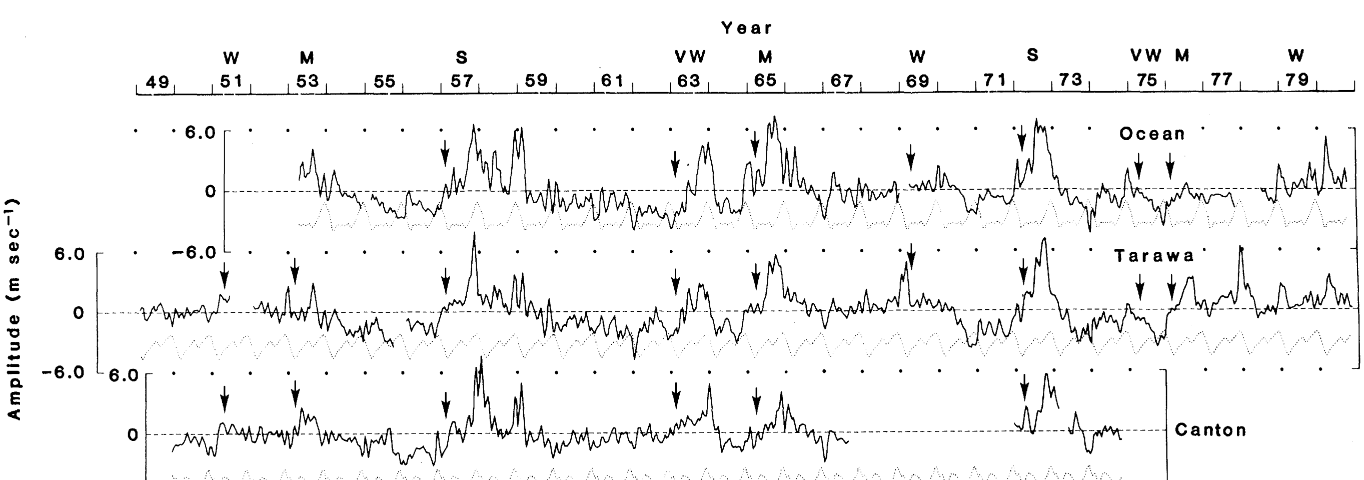

Fig. 1. Low-pass-filtered (14) zonal wind anomalies (continuous lines) recorded at Ocean, Tarawa, and Canton islands. The long-term mean annual cycles that have been subtracted are also plotted (dotted lines). The El Niño events of 1950 to 1978 are indicated in accordance with the classifications of Quinn *et al.* (15): strong (*S*), moderate (*M*), weak (*W*), and very weak (*VW*). In addition, the weak El Niño of 1979 is shown. The arrows indicate the dates of the first warm SST anomalies at the coast of Peru for each El Niño (3, 18–20). Gaps indicate missing data, although the width of each gap is exaggerated by truncation by the low-pass filter.

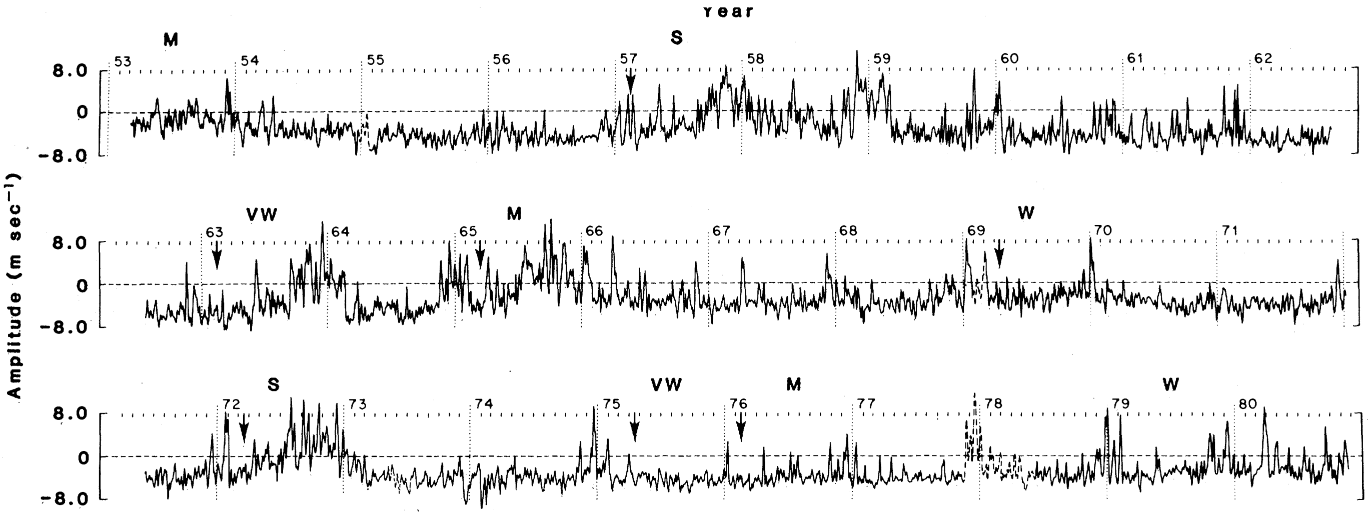

Fig. 2. Low-pass-filtered (*23*) zonal winds at Ocean Island. Gaps due to missing data (January 1955, February 1969, and November 1977 through May 1978) are filled with data from Tarawa. The mean annual cycle has not been removed. The El Niño events and dates of the first warm SST anomalies at the coast of Peru for each El Niño are indicated as in Fig. 1.

equatorial Pacific near the date line, or perhaps by (as yet unobserved) wind anomalies elsewhere along the equator.

The easterly winds at Canton, Tarawa, and Ocean in Fig. 1 increase in strength, as Wyrtki (*3*) suggested, during the year before some El Niño events. The duration of the strong antecedent easterlies is variable and not necessarily related to the magnitude of the subsequent El Niño. More than 2 years of strong easterlies preceded the very weak 1963 El Niño, and less than 1 year of strong easterlies preceded the moderate 1965 El Niño.

The precursive wind changes tend to be much smaller than the subsequent collapse of the easterly winds during the mature phase (*2*) of El Niño. The occurrence of these massive westerly anomalies 9 months to 1 year after the precursor anomaly of each El Niño has overshadowed and confused detection of the precursor anomaly, especially in studies based on seasonal averages (*22*) or correlation analyses (*10, 18*).

Less strongly filtered (*23*) zonal wind (not wind anomaly) data for Ocean Island are shown in Fig. 2. The low-frequency westerly anomalies of Fig. 1 are composed largely of short pulses (days to weeks) of strong westerly winds. Canton and Tarawa exhibit similar structure, but Ocean has the pulses of largest amplitude on average. The pulses occur in most years, but the frequency and magnitude of strong pulses are highly correlated with the El Niño years (Fig. 3).

The oceanic Kelvin wave response to these wind fluctuations of short time scales will be different than for a more slowly varying forcing (*7, 24*); Kelvin waves should be excited and be able to propagate to the eastern boundary. Nonlinear horizontal advection of the existing temperature field by a succession of such downwelling waves can produce a substantial SST anomaly. Philander (*7*) demonstrated numerically that "even weak eastward winds for a short period can cause disproportionately large temperature increases (because of nonlinear mechanisms)." Furthermore, since the wind pulses may excite a variety of Kelvin waves with different vertical scales (*25*), each burst may force waves with different zonal group velocities. These waves will arrive at a given longitude at different times, thus spreading the formation of the SST anomaly in time (*8*). Rossby wave reflection at the eastern boundary can help spread westward the low-frequency components of the coastal anomaly. Therefore, westerly wind bursts over the central and western Pacific could produce a substantial fraction of the observed coastal and equatorial monthly SST anomalies.

The origin of the precursive westerly wind pulses evident in Fig. 2 is not clear. They may be abnormal eastward extensions of the monsoon winds of the far western Pacific, abnormal northward excursions of westerly wind pulses found between 5°S and 10°S during austral spring, or surges of the northeast trades that turn eastward as they cross the equator. The latter process is the least likely since no equatorward anomalies are observed, prior to El Niño events, at island stations north of the equator in the western Pacific (*11*). Later in the El Niño years the trade wind surges can be important, however (*26*).

Once the westerly winds are established at the equator with their concomitant low-pressure troughs in each hemisphere, they may be further enhanced by the formation of cyclones in each trough at nearly coincident times (*26*). For example, the four westerly pulses of November 1977 through January 1978 in

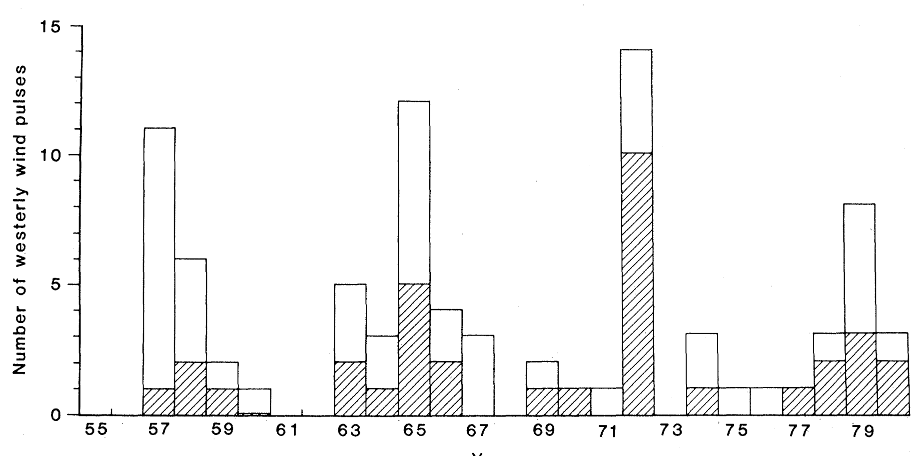

Fig. 3. Number of wind events at Ocean in which a westerly wind (16-hour average) exceeded 8 m sec^{-1} (open bars) and 10 m sec^{-1} (shaded bars).

Fig. 2 have each been explicitly associated with the formation of cyclones in both hemispheres (26).

Identification of westerly wind bursts in the central equatorial Pacific before El Niño events of the past does not improve our capability to predict future El Niño events, beyond what can already be accomplished from monitoring the southern oscillation (27, 28). The strong zonal wind bursts near the date line are neither necessary (for example, there were no bursts before the 1963 El Niño, and very weak bursts occurred before the 1976 El Niño) nor sufficient (for example, strong bursts in 1974 and 1977 were not followed by significant El Niño events) for the existence of El Niño. Other factors, beyond the fluctuations of equatorial winds near the date line, must be influencing the onset and development of El Niño.

D. S. LUTHER
Scripps Institution of Oceanography, La Jolla, California 92093
D. E. HARRISON
Department of Meteorology and Physical Oceanography, Massachusetts Institute of Technology, Cambridge 02139
R. A. KNOX
Scripps Institution of Oceanography

References and Notes

1. C. S. Ramage and A. M. Hori, *Mon. Weather Rev.* **109**, 1827 (1981).
2. E. Rasmusson and T. Carpenter, *ibid.* **110**, 354 (1982).
3. K. Wyrtki, *J. Phys. Oceanogr.* **5**, 572 (1975).
4. J. D. Horel and J. M. Wallace, *Mon. Weather Rev.* **109**, 813 (1981); H. van Loon and R. A. Madden, *ibid.*, p. 1150.
5. J. McCreary, *J. Phys. Oceanogr.* **6**, 632 (1976).
6. H. E. Hurlburt, J. C. Kindle, J. J. O'Brien, *ibid.*, p. 621.
7. S. G. H. Philander, *ibid.* **11**, 176 (1981).
8. P. S. Schopf and D. E. Harrison, *ibid.* **13**, 936 (1983).
9. T. P. Barnett, *ibid.* **7**, 633 (1977).
10. It is well known (2, 3) that months after El Niño begins the equatorial trade winds completely collapse, giving rise to a second peak in the SST anomaly at Peru.
11. D. S. Luther and D. E. Harrison, *Mon. Weather Rev.*, in press.
12. A. J. Busalacchi and J. J. O'Brien, *J. Geophys. Res.* **86**, 10901 (1981).
13. The possible importance of energetic westerly wind bursts to the development of El Niño has been suspected for many years (G. Meyers, personal communication).
14. The wind data have been low-pass-filtered by a cosine sum filter with the point at −3 dB at 70 days and the point at −10 dB at 50 days. The series were subsequently decimated to approximately 1 point for every 14 days, and the long-term mean annual cycle was subtracted.
15. W. H. Quinn, D. O. Zopf, K. S. Short, R. T. W. Kuo Yang, *Fish. Res. Bull.* **76**, 663 (1978).
16. J. R. Donguy, A. Dessier, G. Meyers, *Trop. Ocean-Atmos. Newsl.* **16**, 7 (1983).
17. W. S. Wooster, *ibid.*, p. 4.
18. B. Hickey, *J. Phys. Oceanogr.* **5**, 460 (1975).
19. K. Wyrtki, *ibid.*, **9**, 1223 (1979).
20. J. Namias, *ibid.*, **6**, 130 (1976).
21. The Kelvin wave phase and group speeds vary from 2.3 m sec^{-1} in the eastern Pacific to 3.0 m sec^{-1} at the Gilbert Islands for the first baroclinic mode, and from 1.3 to 1.7 m sec^{-1} for the second baroclinic mode [D. S. Luther, thesis, Massachusetts Institute of Technology, Cambridge (1980)].
22. S. E. Pazan and G. Meyers, *Mon. Weather Rev.* **110**, 587 (1982).
23. The point at −3 dB is now 9 days and the point at −10 dB is 6 days.
24. S. G. H. Philander and R. C. Pacanowski, *J. Geophys. Res.* **86**, 1903 (1981).
25. ———, *ibid.* **85**, 1123 (1980) concluded that the dominant vertical scale will be similar to that for a second baroclinic mode, where the fluctuation is trapped somewhat to the surface layers by reflection at the thermocline.
26. R. A. Keen, *Mon. Weather Rev.* **110**, 1405 (1982).
27. W. H. Quinn, *J. Appl. Meteorol.* **13**, 825 (1974).
28. W. Wyrtki, E. Stroup, W. Patzert, R. Williams, W. Quinn, *Science* **191**, 343 (1976).
29. We thank J. W. D. Hessel and colleagues of the New Zealand Meteorological Service for supplying manuscript copies of the Gilbert Islands data. The U.S. National Climatic Center supplied the Canton Island record. S. Pazan was instrumental in obtaining the Gilbert Islands data, which J. Bytof digitized and preprocessed. Supported by NSF Pacific Equatorial Ocean Dynamics (PEQUOD) program grants OCE 79-21836 (Scripps Institution of Oceanography) and 79-21815 (Massachusetts Institute of Technology). This is PEQUOD contribution 21. Additional funds (for keypunching) were supplied under the Equatorial Pacific Ocean Climate Studies program of the National Oceanic and Atmospheric Administration.

5 July 1983; revised 22 August 1983

Fluoride Directly Stimulates Proliferation and Alkaline Phosphatase Activity of Bone-Forming Cells

Abstract. *Fluoride is one of the most potent but least well understood stimulators of bone formation in vivo. Bone formation was shown to arise from direct effects on bone cells. Treatment with sodium fluoride increased proliferation and alkaline phosphatase activity of bone cells in vitro and increased bone formation in embryonic calvaria at concentrations that stimulate bone formation in vivo.*

Fluoride is essential in the diet and is thought to be required for normal dental and skeletal growth (1). The recommended allowance of fluoride is 1 to 4 mg per day. Doses of 20 to 100 mg per day, or more, usually cause abnormal increases in skeletal mass, even to the point of sclerosis (2). This may represent an exaggerated physiological response or a new and unrelated action, but because the effect of excess fluoride is selective for bone, it has therapeutic applications. Clinical studies have shown that NaF is the most potent agent for increasing bone volume in patients with osteoporosis (3, 4). Although the mechanism is unknown, the skeletal response to supplemental NaF is characterized by increases in (i) the rate of bone formation (4, 5); (ii) the number of osteoblasts, or bone-forming cells (4, 6); and (iii) the serum activity of skeletal alkaline phosphatase (ALP) (7–9), an osteoblastic isoenzyme.

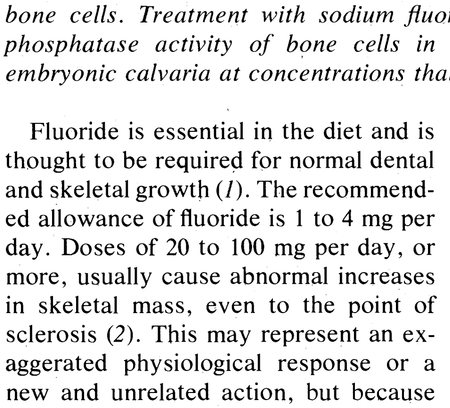

Fig. 1. Dose-response curve for fluoride. Calvarial cell proliferation estimated as [^{3}H]thymidine incorporation, shown as percent of control (no fluoride), versus NaF concentration. Values represent the mean ± S.E.M. of six replicates. Dashed line indicates the mean of the control values. A single asterisk indicates a significant difference from controls at $P < 0.05$; a double asterisk indicates $P < 0.005$.

To discover the mechanism whereby fluoride stimulates bone formation, we sought (i) to determine whether any of the characteristic skeletal responses to NaF could be attributed to direct effects on cells in the osteoblast line and (ii) to examine the interactions between NaF and two other bone cell mitogens—parathyroid hormone (PTH) and human skeletal growth factor (hSGF) (10–13). To these ends we have examined the effects of NaF on embryonic chick bone cells in vitro and on embryonic chick bone in organ culture (14, 15).

Bone cells for these studies were prepared from the calvaria of 15-day embryonic chicks by sequential collagenase digestion and were cultured in serum-free Fitton-Jackson modified BGJ_b medium (16). Histological analysis of the calvaria before digestion has shown that essentially all of the cells available for release were members of the osteoblast cell line. Even in monolayer culture these cells maintained the following characteristics of osteoblasts and osteoblast progenitors: expression of a skeletal-type ALP activity; response to PTH with an increased adenosine 3′,5′-monophosphate (cyclic AMP) production (11); conversion of 25-hydroxyvitamin D_3 to more polar metabolites (17); and response to a bone-derived mitogen (hSGF) that is specific for skeletal tissues (12, 13).

To estimate cell proliferation we incubated the calvarial cells overnight and then exposed them to effectors (such as NaF and hSGF) for an additional 18 to 24 hours [this corresponds to the cell cycle